Analysing the Dynamic Stabilization of Aluminium Electrolysis Cells

Marc Dupuis[1] and Valdis Bojarevics[2]
1. Consultant
GeniSim, Jonquière, Canada
2. Professor
University of Greenwich, London, United Kingdom
Corresponding author: marc.dupuis@genisim.com
https://doi.org/10.71659/icsoba2025-al086

Abstract

It was demonstrated in [1], by using the MHD-Valdis code to perform non-linear transient cell stability analysis, that it is possible to stabilize an aluminium electrolysis cell by alternating the potline current. This stabilization effect is highly dependent on the cell operating parameters, such as anode-to-cathode distance (ACD) and cell dimensions, and the alternating current amplitude and frequency. Later it was demonstrated in [2], still using the MHD-Valdis code that it is also possible to stabilize an aluminium electrolysis cell by alternating the current in magnetic field compensation busbar loops only.

A very large number of combinations of parameters exist, and it would be ideal to find the optimal combination for the most efficient stabilization. However, each simulated combination of alternating current and cell parameters requires an overnight run, limiting the number of analysed combinations in a week per example to only a few. Having a reduced model where it would be possible to explore the stability of the cell of a great number of combinations very quickly would be of great benefit in reducing the total number of MHD-Valdis simulations that we need to run to find the optimum combination. For example, a detailed frequency vs amplitude stability map was produced in [3, 4] using a frictionless mechanical pendulum model.

However, the pendulum model did not exhibit stability and instability at realistic cell parameters. This limits the map's usefulness in identifying parameter combinations of interest to investigate using the MHD-Valdis model for a real cell. A damped mechanical mobile model [5, 6], that more closely mimics behaviour an actual aluminium reduction cell to investigate the cell stability was developed to address that limitation.

In the present work, both the damped mechanical mobile model and MHD-Valdis code are used to further investigate the frequency vs amplitude stability map of dynamic stabilization by alternating the current in magnetic field compensation busbar loops.

Keywords: Magnetohydrodynamic instability, Aluminium cell modelling.

1. Introduction

Magneto-Hydro-Dynamic (MHD) cell stability is a complex phenomenon that involves electric energy transfer into mechanical energy through a mechanism of resonance. Peter Davidson developed his pendulum mechanical model to illustrate that mechanism of resonance [7].

Urata explained the wave mechanism in [8], the main ingredient for rotating wave amplification is a longitudinal gradient of the vertical component of the magnetic field (x component of gradient of Bz). The second ingredient is the magnitude of the horizontal components of the metal pad current density in both the longitudinal and transversal directions (Jx and Jy).

To optimize MHD cell stability, the busbar network layout is designed in order to minimize overall Bz component. The busbar network is also balanced in order to minizine Jx and the cathode assembly is designed in order to minimize Jy. In old cell designs, external magnetic field compensation busbar loops can be added to minimize Bz without modifying the existing busbar or in new cell designs rely on external compensation busbar loops in order to minimize busbar network weight, hence the busbar cost.

In [1] a totally new way to increase MHD cell stability was proposed: alternating potline current. By alternating the potline current, a new wave is generated that is interfering with the growth of the naturally occurring rotating wave; in reference [4] this effect is called anti-resonance. It was demonstrated in [1] using MHD-Valdis code that anti-resonance by alternating the potline current is increasing cell stability. In [2], it was also demonstrated that anti-resonance by alternating the current in compensation busbar loops is increasing cell stability. In [3], the Davidson frictionless pendulum model was extended to demonstrate analytically that anti-resonance by alternating the model current density parameter (potline current) is working. A frequency/amplitude map was produced. That mathematical work on Davidson pendulum model was reproduced and extended in [4].

The problem with the Davidson frictionless pendulum model is that even if its behaviour is analogous to real cells, the stability threshold is very different from real cells, so the stability map produced is not useful to indicate what would be the most efficient frequency/amplitude combination for those real cells. Unfortunately, direct usage of MHD-Valdis to investigate a real cell frequency/amplitude stability map is very CPU time consuming so for this reason, it is not very practical.

For those reasons, a damped mechanical mobile model was developed [5, 6]. That new mechanical model once calibrated instantaneously provides a wave damping rate very similar to the one that can be calculated after an MHD-Valdis overnight run. The variation of ACD and potline current stability map of conventional cell operation was quickly obtained using that mechanical model. The present work is an extension of the work presented in [2] and [6].

2. Third Calibration of the Damped Mechanical Mobile Model

In [5] a first calibration of the mobile model was presented. That first calibration led to a first prediction of the damping rate for a change of ACD that was looking promising but was not so close to the wave damping rate obtained by MHD-Valdis. For that reason, in [6], a second calibration was performed that led to the production of damping rate very close to those obtained by MHD-Valdis as presented in figure 11 of [6].

The two model parameters that are adjusted to match one damping rate prediction of MHD-Valdis are n, the relative position of the centre of mass of the mobile aluminium plate and ζ, the plate motion damping coefficient. There is a multitude of combinations of those two parameters that leads to the reproduction of a single damping rate obtained from MHD-Valdis, but in fact the two parameters can be used to reproduce two MHD-Valdis results. Table 1 compare the results obtained with the 2nd and 3rd calibration with the ones obtained with MHD-Valdis. The calibrated results are displayed in bold. Obviously, it is possible to calibrate using any combination of two results obtained by MHD-Valdis. The new results are not that different from those presented in figures 4 and 5 of [6] which is a good thing. The hope is that this new calibration method could be use systematically for other cell designs in the future.

The results of the damped mobile model are obtained using a MATLAB App developed by Ibrahim Mohammad. Figure 1 presents the results obtained for the second calibration point. The model setup parameters are entered and by pressing “Solve” the damping rate is calculated and

the graph showing the plate oscillation is produced. The damping rate of MHD-Valdis results are also calculated using a MATLAB App developed by Dr. Ibrahim Mohammad, Figure 2 presents the results obtained processing the initial "base case" results. The App read the file produced by the MHD-Valdis overnight run, process the data and display the result.

Table 1. Comparison of MHD-Valdis damping rate results with those obtained using the 2nd and 3rd calibration of the mobile model.

J_0 (A/cm^2)	ACD (cm)	Rate (/s) MHD-Valdis	Rate (/s) 2nd calibration	Rate (/s) 3rd calibration
0.80	4.3	0.00007	**0.00000**	**0.00000**
0.80	4.5	-0.00199	-0.00179	-0.00209
0.80	4.0	0.00352	0.00301	**0.00352**
0.72	4.3	-0.01154	-0.01037	-0.01040
0.72	4.0	-0.00853	-0.00762	-0.00718
0.84	4.5	0.00312	0.00326	0.00296
0.84	4.3	0.00477	0.00512	0.00513

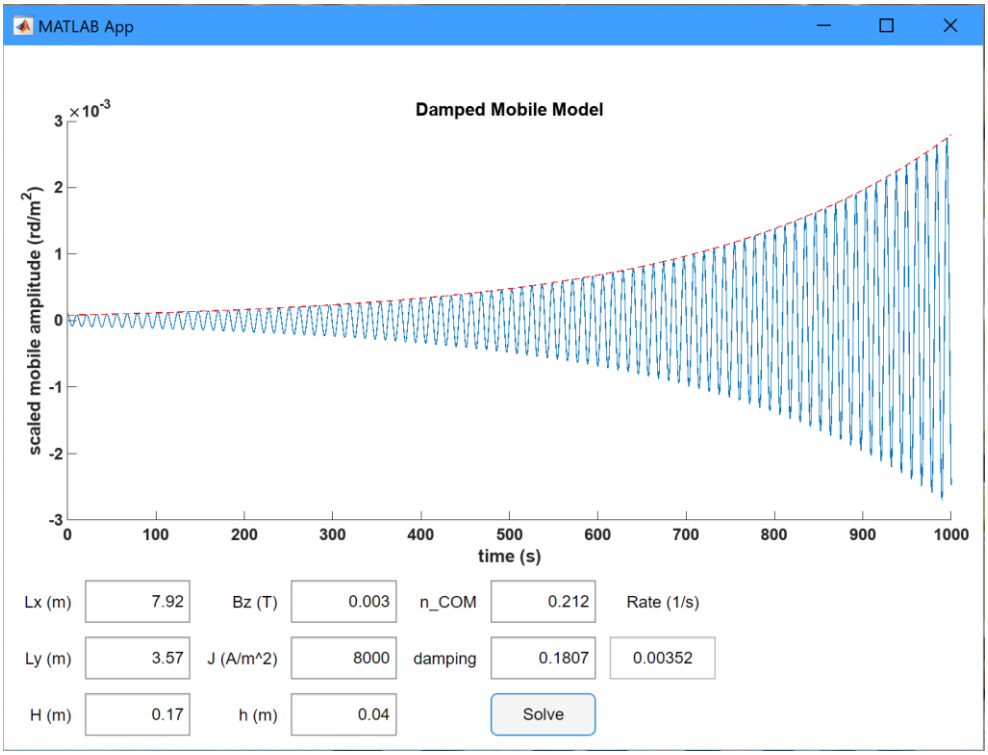

Figure 1. Mobile plate displacement at $J_0 = 0.8$ A/cm^2 and 4.0 cm ACD. The mobile is unstable with the exponent 0.00352 /s.

3. Testing Prediction of the Mobile Model to a Change of Magnetic Field

One of the mobile model parameters is Bz; it was set to 30 G for the model calibration. It is supposed to represent the "average" magnetic field on one side of the cell. In real cells, the magnetic Bz is not constant, and it is usually not possible to change only the magnetic field to be able to produce a comparison result using MHD-Valdis. But with the usage of compensation busbar loops, it is possible to modify only the Bz in MHD-Valdis. Figure 3 presents the Bz without compensation busbar loops on top and at bottom with 20 kA passing in each of the two compensation busbar loops.

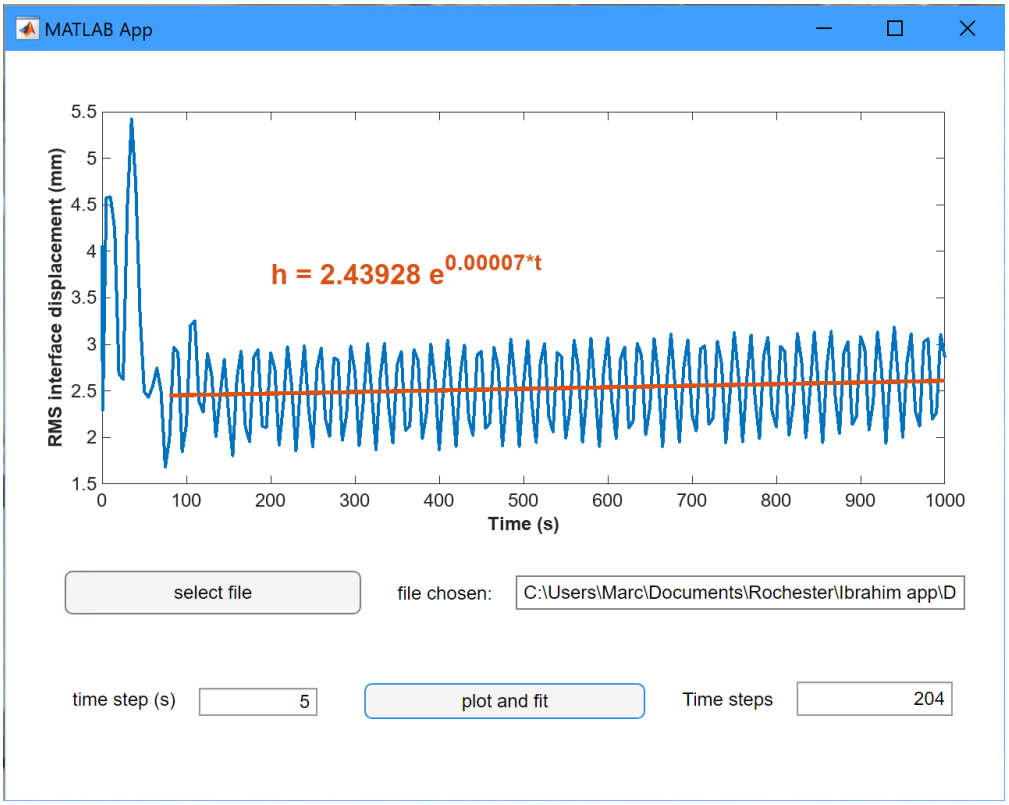

Figure 2. RMS interface displacement at $J_0 = 0.8$ A/cm^2 and 4.3 cm ACD. The cell is critically stable with the exponent ~ 0.

The Bz is very large in the two upstream cell corners, around -60 G in the left upstream corner to +70 G in the right upstream corner. But it is close to zero in the two opposite downstream corners. Hence the choice of using 30 G as Bz in the mobile model. The compensation busbar loops bring the left side up and push the right side down. Instead of trying to assess the new Bz for the mobile model, it was decided to look for the value that reproduces MHD-Valdis prediction of the gained stability. Figure 4 presents the stability results obtained, on the left from MHD-Valdis and on the right the mobile model result. To get the same damping rate in the mobile model, you need to replace Bz from 30 G to 22.7 G. This looks reasonable but this is more a qualitative comparison exercise than a quantitative one unfortunately.

4. Using the Mobile Model to Explore Dynamic Alternating Line Current Frequency vs Amplitude Stability Map

We have seen in [3, 4] the frequency vs amplitude stability map produced by the frictionless pendulum model. That map is complex and is of little to no utility to identify interesting region to explore in a real cell using MHD-Valdis code while it is not practical to directly explore the full map using that code as each point on the map requires an overnight run to compute.

As we can see in Figure 5a, the natural frequency of this plate oscillation is about 0.0775 Hz, corresponding to a period of 12.9 s. Unfortunately, this frequency is much higher than the natural frequency of the MHD wave it is supposed to represent. So, we need to use natural wave frequency multiples. Let us try first 1x at 0.0775 Hz. Figure 5b presents the results for 1x, the natural wave at the maximum amplitude of the full line current. This is the most effective amplitude at that frequency, and the maximum amplitude the App accepts. The damping rate is calculated to be -0.00365 /s. At 0.11625 Hz or 1.5x frequency, the damping rate is -0.01047 /s. At 0.155 Hz or 2x frequency, the damping rate is -0.01450 /s. At 0.1938 Hz or 2.5x frequency,

the damping is back to -0.00234 /s as we can see in Figure 5c. Figure 1d shows that the maximum damping rate of -0.02542 occurs at 0.1542 Hz frequency (1.99x) and changes very rapidly around that frequency. While using dynamic stabilization at the 0.1542 Hz frequency and 1x amplitude, the ACD needs to be reduced to 3.855 cm before critical stability is reached again.

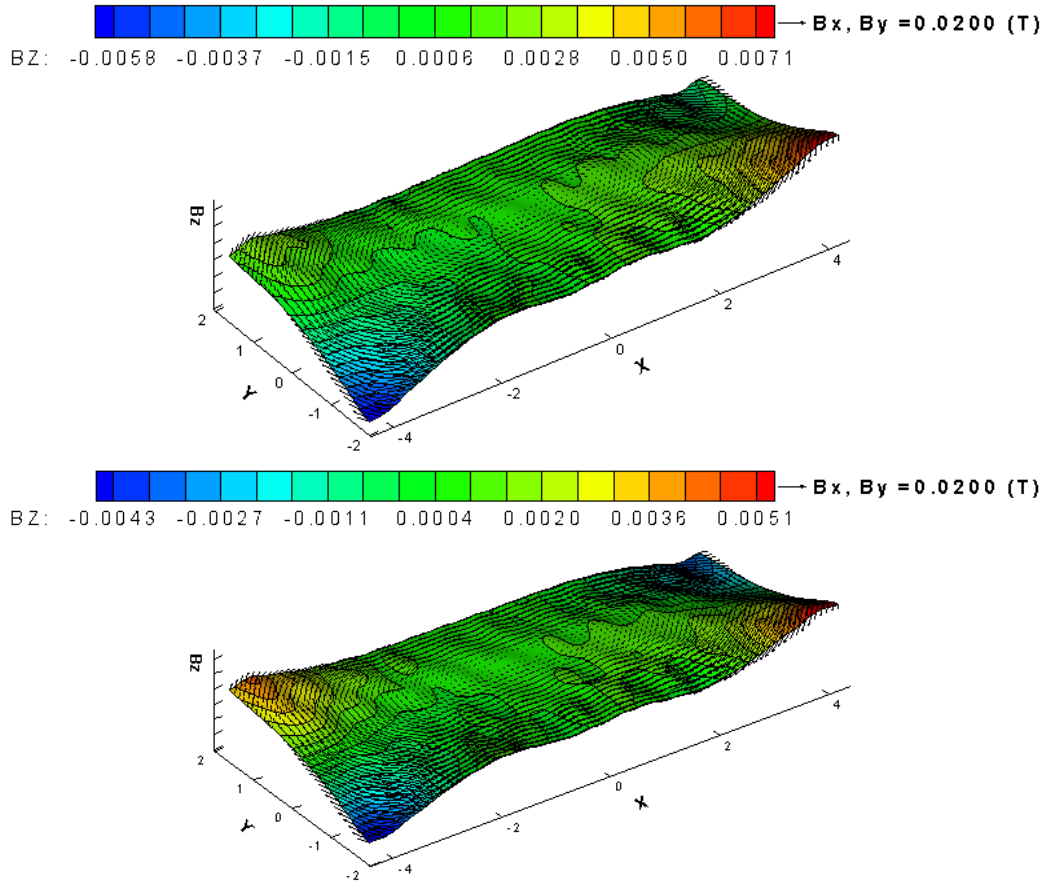

Figure 3. Bz without compensation loops on top and with 20 kA passing in each of the two compensation loops below.

The frictionless pendulum model and the damped mobile model can only analyse the effect of alternating the potline current, but as it was argued in [2] that it would be quite challenging for a smelter to implement this mode of dynamic compensation. Furthermore, an amplitude of 1 time the line current means alternating the potline current at the amplitude of the nominal potline current, it would certainly not be possible to use such a big amplitude in a real cell. So, the knowledge gained by using the damped mobile model is that dynamic stabilization maximum efficiency occurs at about two times the natural wave frequency and at the maximum possible amplitude.

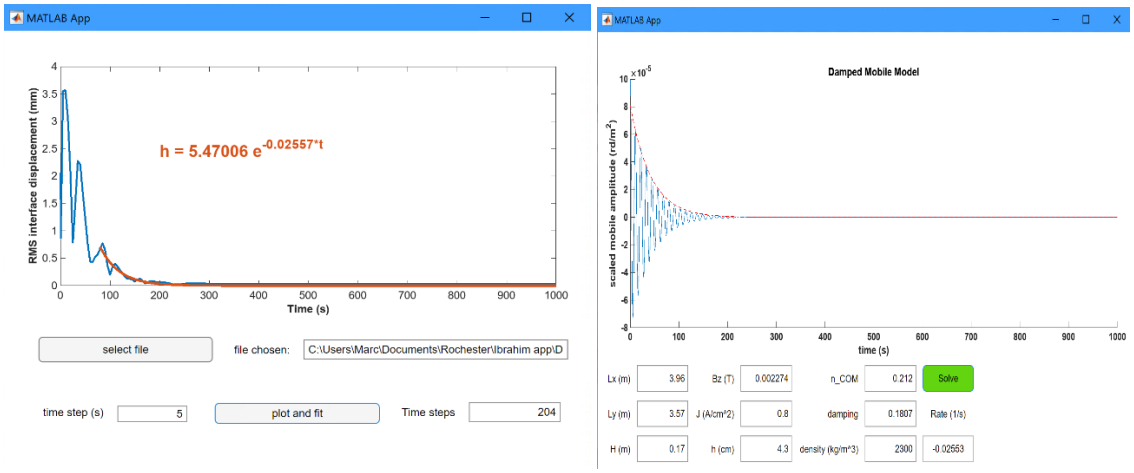

Figure 4. Cell stability wave damping rate prediction after reduction of Bz, left MHD-Valdis results, right mobile model results.

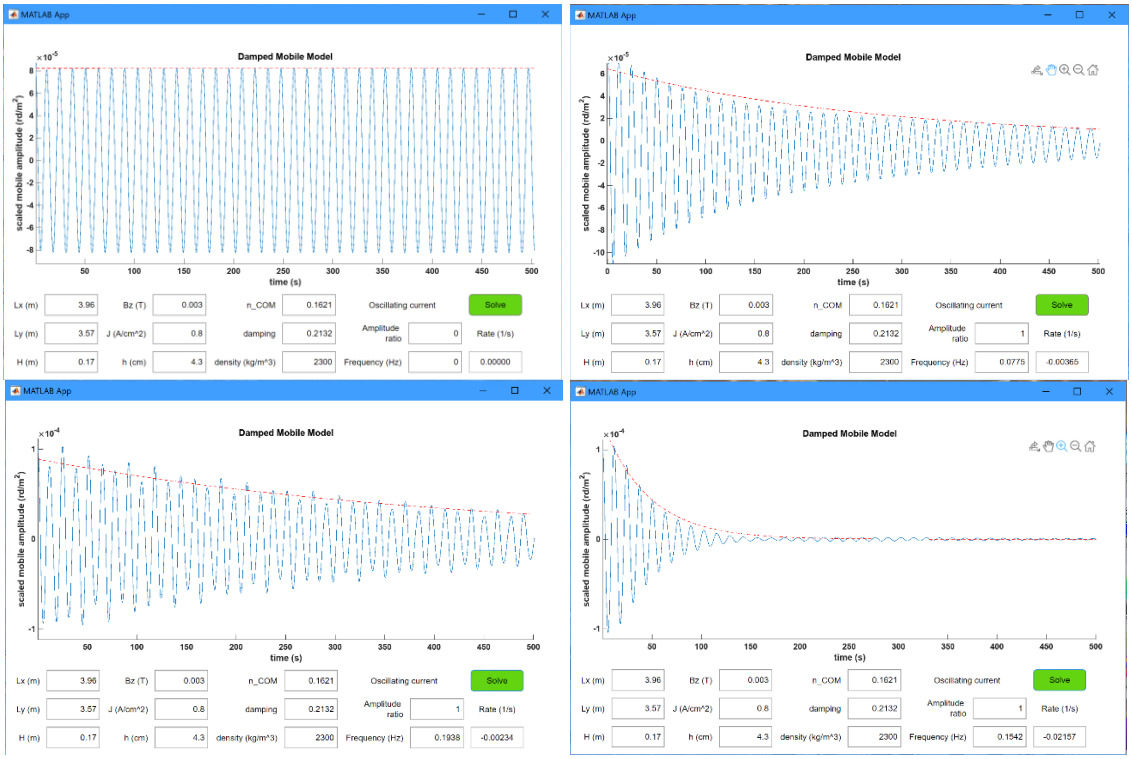

Figure 5. Evolution of the damping rate at different alternating line current frequencies. 5a top left: without current oscillation, 5b top right: at 1x, the natural plate oscillation frequency, 5c bottom left: at 2.5x, 5d bottom right: at about 2x.

5. Investigation of the Dynamic Stabilization by Alternating the Current in Magnetic Field Compensation Busbar Loops Using MHD-Valdis

Since MHD-Valdis can investigate both dynamic stabilization by alternating the full potline current and by only alternating the current in compensation busbar loops, and since it was previously demonstrated that both are increasing the cell stability, it was decided to continue to investigate the second method in the present work as this method would be more practical to implement in smelters.

5.1 Selection of the Most Efficient Static Compensation Current

The usual way to use compensation busbar loops is to use a constant current to reduce the Bz and hence increase the cell stability. As presented in Figure 3 and 4, passing 20 kA in the two compensation busbar loops significantly improves the Bz and cell stability. Now, we have a way to quantify that improvement. According to MHD-Valdis results, the damping rate goes from -0.00007 to -0.02557 /s. Figure 6 presents results when 30 kA is passed instead, the damping rate is even more pronounced at -0.02741 /s, so 30 kA static compensation is better that 20 kA static compensation.

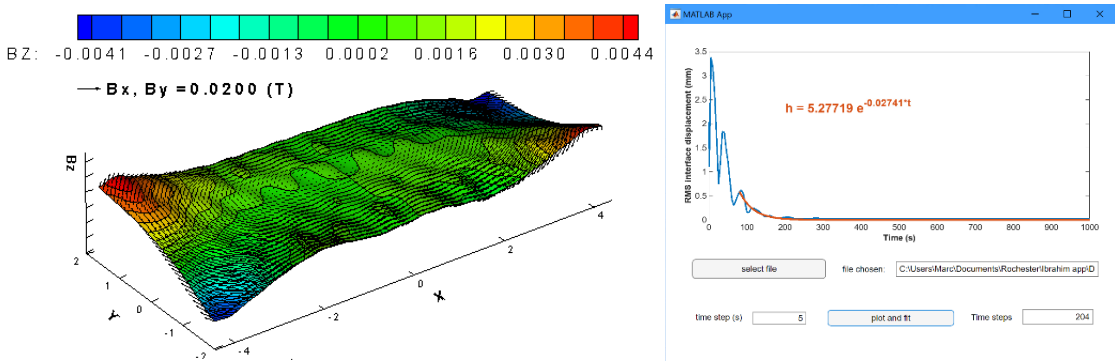

Figure 6. Results with 30 kA current in compensation loops. Left: Bz, Right: Resulting damping rate.

5.2 Testing the Effect of Changing Dynamic Compensation Frequency

Since it is not possible to fully explore the frequency/amplitude stability map using MHD-Valdis, this study will limit itself to verifying the insights obtained with the damped mobile model. First insight was that 2 times the natural wave frequency (1x) is the most efficient antiresonance frequency (2x). Three frequencies were tested, respectively 2 times (2x), 3 times (3x) and 4 times (4x) the natural wave frequency (1x) which is 0.02463 Hz, corresponding to a period of 40.6 s. Because of the 0.1 s time step size, which was selected to better accommodate frequency selection, 2x frequency was setup using a 20.3 s period so 0.04926 Hz. The 3x frequency was setup using a 13.5 s period so 0.0741 Hz, and finally the 4x frequency was setup using a 10.1 s period so a 0.099 Hz frequency.

This is surely a very small frequencies sample, which will for sure not tell the full story, per example fraction of the natural wave frequency were not tested like 2.5x etc. Also, the high sensitivity of the damping rate around 2x frequency observed in the damped mobile model was not investigated using MHD-Valdis. Unfortunately, a more serious probing of the frequency/amplitude map using MHD-Valdis would take months of CPU time.

Figure 7 presents the results for the 3x frequency on the left and 4x frequencies on the right using a 10 kA amplitude with min and max at 25 and 35 kA with the ACD reduced to 3.9 cm. Results of 2x frequency with the same 10 kA amplitude with min and max at 25 kA and 35 kA and also with 3.9 cm ACD are presented on the left side of Figure 8.

The resulting damping rates are -0.00640 /s at 2×, -0.00303 /s at 3x and -0.00711 /s at 4×. The 4× antiresonance frequency is essentially not excited, so, it is like using static compensation at 30 kA. The 2x frequency works better than the 3× frequency, confirming the damping mobile model results. At 3.9 cm ACD, the static compensation at 30 kA is working better than the 2× frequency 10 kA amplitude dynamic compensation because the dynamic compensation generates a stable wave residual not present in static compensation.

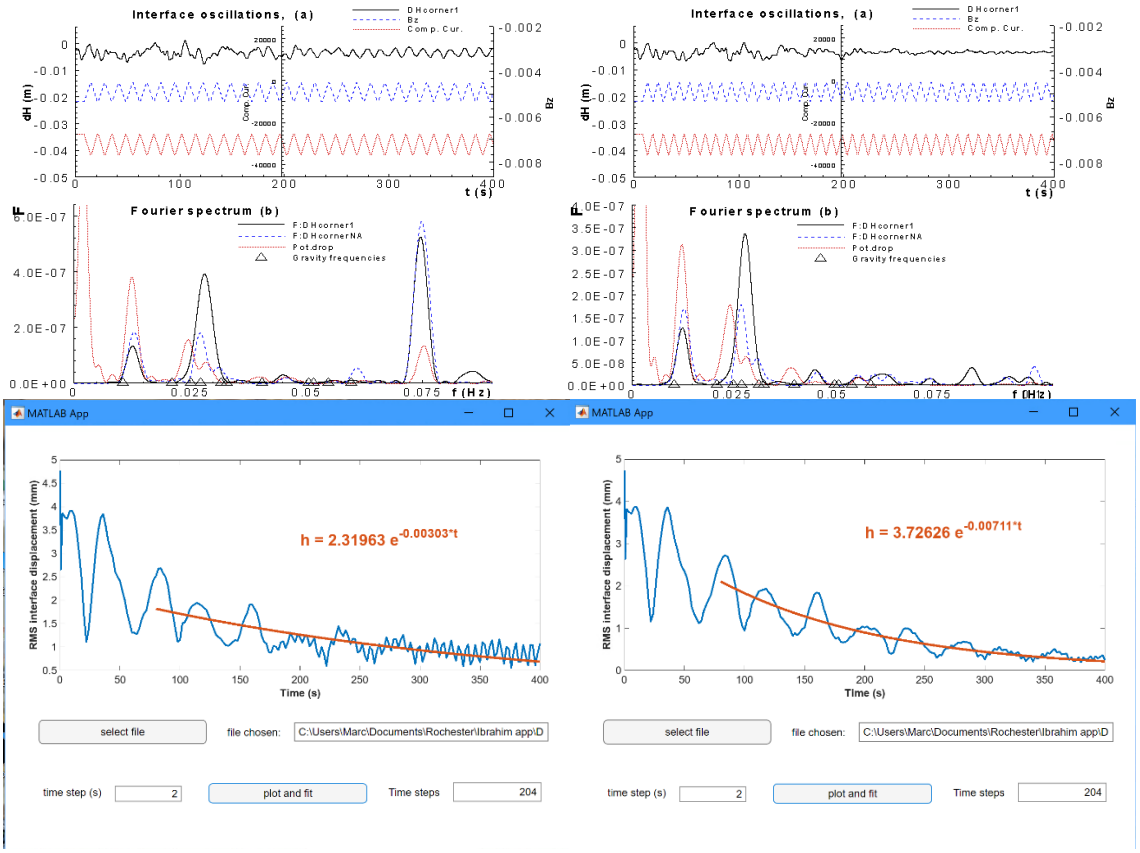

Figure 7. Results with alternating current in compensation loops, both from 25 to 35 kA. Left: at 0.0741 Hz (3x), Right: at 0.099 Hz (4x).

5.3 Testing the Effect of Changing Dynamic Compensation Amplitude

Again, since it is not possible to fully explore the frequency/amplitude stability map using MHD-Valdis, the study will limit itself to verifying the insights obtained with the damped mobile model. Second insight was that greater amplitude is more efficient. Two amplitudes were compared. Figures 8 left side present the results when the ACD is reduced to 3.9 cm with dynamic compensation at 0.04926 Hz which is 2 times the natural wave frequency (1x). In that case, the amplitude is 10 kA with min and max at 25 and 35 kA and in the other case in Figures 8 right side, the amplitude is doubled at 20 kA with min and max at 20 and 40 kA, hence in the two cases, the average compensation remained at the optimum 30 kA compensation value. Figures 8 also shows the damping rate obtained, with 10 kA, the amplitude the damping rate is -0.00640 /s and with 20 kA amplitude, the damping rate is -0.00563 /s. This result is in contradiction with what was observed using the damped mobile model. This might be explained by the fact that by oscillating the current in the compensation busbar loops, we are moving away from the optimum compensation position in both directions while when oscillating the potline current, half of the time we are decreasing the line current below the nominal value which increases the cell stability.

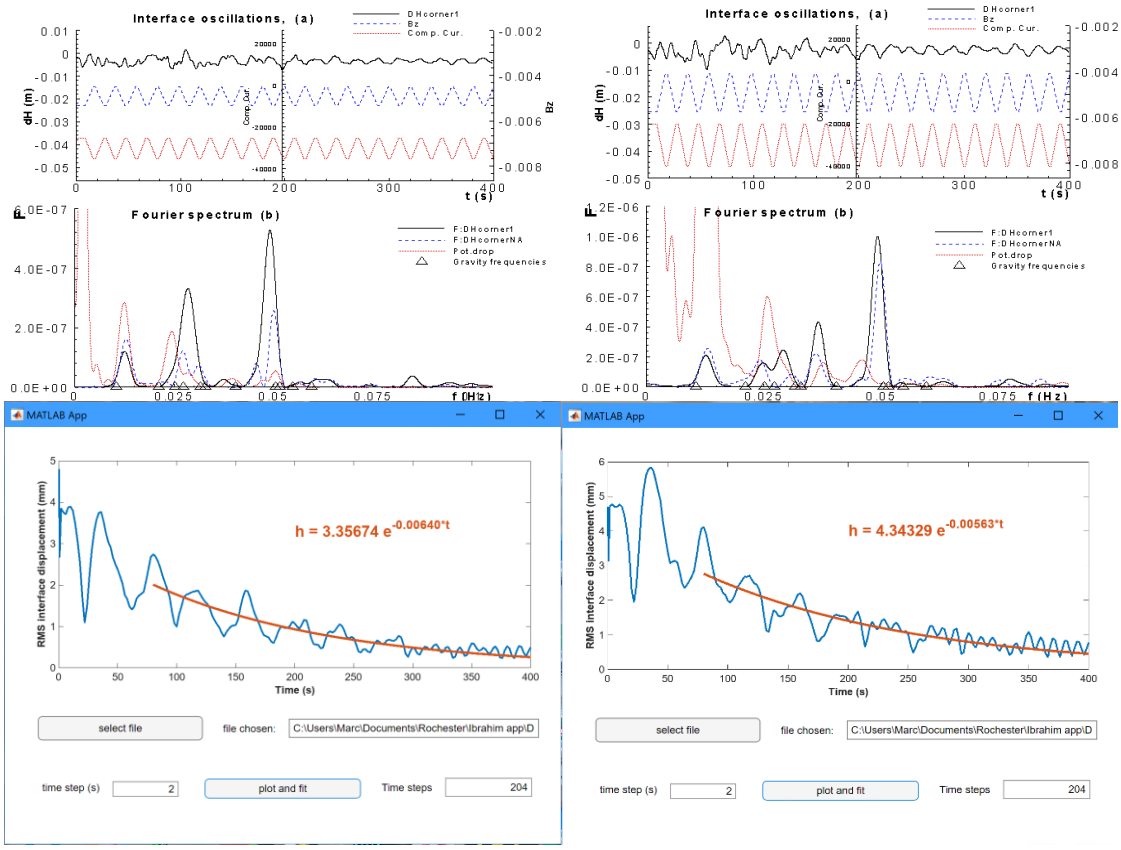

Figure 8. Results with alternating current in compensation busbar loops at 0.04926 Hz (2x). Left: from 25 to 35 kA, Right: from 20 to 40 kA.

6. Finding the ACD to Get Back to Critical Stability Both for Static Compensation Alone and for Combined Static and Dynamic Compensation

As presented in Figure 2, without compensation at all, the 180 kA Hamburg TRIMET cell is predicted to be critically stable at 4.3 cm ACD and 17 cm of metal pad thickness. With constant 30 kA in two compensation loops, it is predicted to be very stable still at 4.3 cm ACD as we can see on the left side of Figure 6. But what is the new minimum where the cell gets back to critical stability with 30 kA static compensation?

In order to answer that question, multiple stability analysis runs were performed at different ACDs. At 3.1 cm ACD the cell is still predicted to be stable but at 3.0 cm ACD, the run stop very early as the metal short-circuit by touching the anode. This is of course not the precise answer and 30 kA static compensation is not necessary the current for optimum compensation but that is a relatively good reference point.

For the dynamic compensation case, the 2x or 0.04926 Hz frequency, 10 kA amplitude with a minimum of 25 kA and a maximum of 35 kA alternating current was established as the best option from the very few combinations tested. This is for sure not the optimum combination, a lot more scanning on the stability map would be required to find that optimum combination. Using that mixed static and dynamic compensation combination, the cell is still predicted to be stable at 2.9 cm ACD as results presented in Figure 9 indicate. Using an even lower ACD was not investigated due to lack of time. Notice the complex shape of the damping curve. it makes the estimation of the damping rate less reliable. It is interesting to notice that the damped mobile model generated similar complex damping shape very close to the optimum damping frequency as we can see in Figure 10.

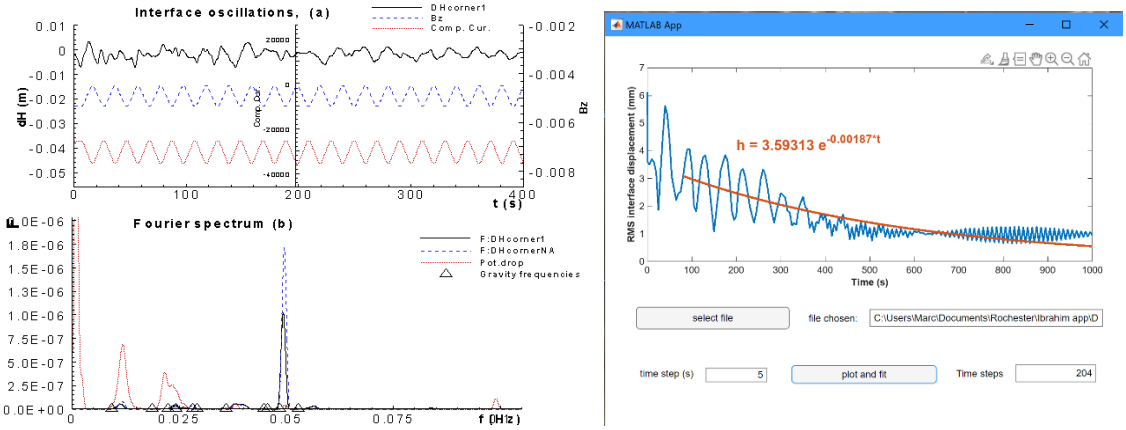

Figure 9. Results with alternating current in compensation loops, from 25 kA to 35 kA at 0.04926 Hz (2x) and 2.9 cm ACD.

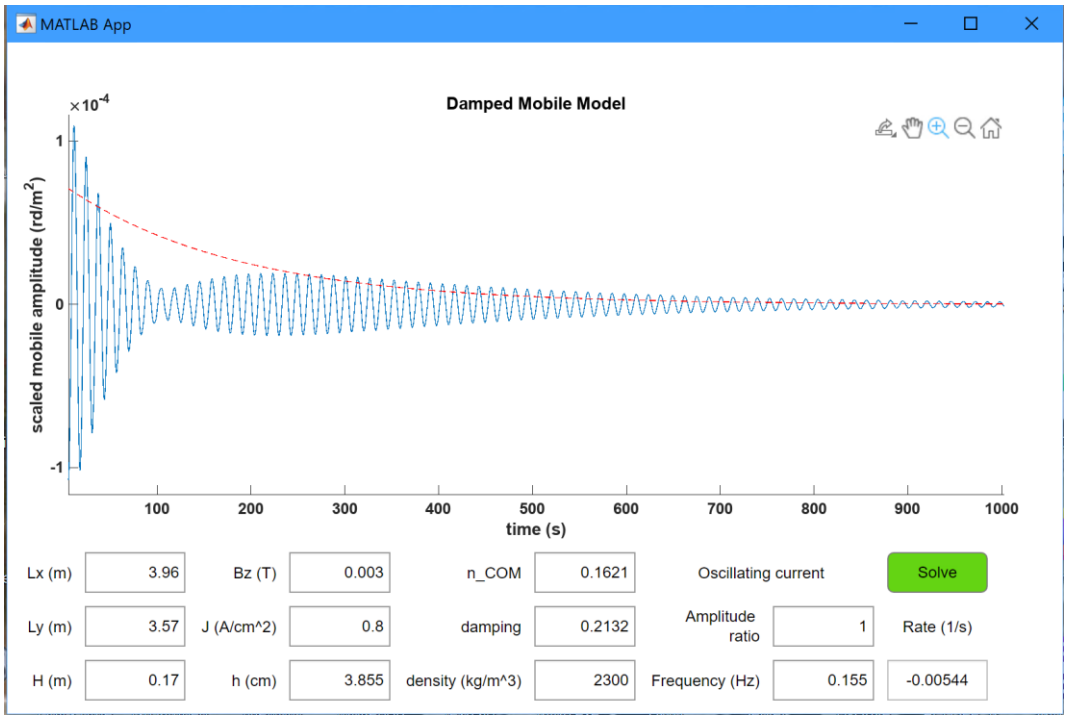

Figure 10. Evolution of the damping rate at 0.155 Hz alternating line current frequency obtained by the damped mobile model at 3.855 cm ACD

7. Conclusions

The damped mobile model was calibrated for the third time in order to use the two calibration parameters n and ζ to reproduce two MHD-Valdis damping rate predictions. The reproduction of MHD-Valdis damping rate for other cases is just marginally better but this new calibration method offers more flexibility as any combination of two MHD-Valdis damping rate results can be used to perform the calibration.

The impact of changing the magnetic field magnitude parameter in the damped mobile model on the damping rate was demonstrated to be qualitatively similar to the one obtained using MHD-Valdis.

According to the damped mobile model, the maximum stabilization effect is obtained using the maximum alternating line current amplitude possible at 2x (twice) the natural plate oscillation frequency.

While using MHD-Valdis to investigate the frequency/amplitude stability map of alternating the current in compensation busbar loops, it was observed that 2x the naturally occurring rotating wave frequency is more efficient than 3x frequency and that 4x frequency is essentially not responding.

While using MHD-Valdis to investigate the frequency/amplitude stability map of alternating the current in compensation busbar loops around the optimum static compensation current, it was observed that 10 kA amplitude is more efficient than 20 kA amplitude.

For the static compensation at 30 kA, the last stable results were obtained at 3.1 cm ACD. For mixed compensation using 2x or 0.04926 Hz frequency, 10 kA amplitude with a minimum of 25 kA and a maximum of 35 kA alternating current, stable results were obtained down to 2.9 cm ACD.

So, static compensation alone has a huge stabilization impact as the critical ACD was reduced from 4.3 cm to 3.1 cm. By adding dynamic compensation, the ACD can be further reduced to at least 2.9 cm.

8. Acknowledgment

The authors would like to acknowledge Dr. Ibrahim Mahammad, professor from Rochester University, for contributing the three MATLAB Apps used in the work presented in this paper.

9. References

1. Ibrahim Mohammad et al., Oscillating currents stabilize aluminium cells for efficient, low carbon production, *JOM* 74, 2022, 1908–1915.
2. Marc Dupuis and Valdis Bojarevics, Stabilizing aluminium reduction cells by oscillating currents in magnetic compensation loops, *Proceedings of 40th International ICSOBA Conference*, Athens, Greece, 10 - 14 October 2022, Paper AL 20, *TRAVAUX* 51, 1243–1254.
3. Ibrahim Mohammad and Douglas H. Kelley, Stabilizing a low dimensional model of magnetohydrodynamic instabilities in aluminium electrolysis cells, *Light Metals* 2022, 512–519.
4. Gerrit Maik Horstmann, Julia Kuhn and Fadi Dohnal, Suppression of magneto-hydro-dynamic interfacial wave instabilities by means of parametric anti-resonance, *Nonlinear Dynamics*, 113(12):14449–14469, February 2025.
5. Ibrahim Mohammad, Marc Dupuis, and Douglas Kelley, A new mechanical model of magnetohydrodynamic instabilities in aluminium electrolysis cells, *Proceedings of 41st International ICSOBA Conference*, Dubai, UAE, 5–9 November 2023, Paper AL52, TRAVAUX 44, 1763–1772
6. Ibrahim Mohammad, Marc Dupuis and Valdis Bojarevics, Analyzing the stability of aluminium electrolysis cells using a mechanical model, *Proceedings of 42nd International ICSOBA Conference*, Lyon France, 27-31 October 2024, Paper AL57, TRAVAUX 45, 1735–1746.
7. P. A. Davidson and R. I. Lindsay, Stability of interfacial waves in aluminium reduction cells, *J. Fluid Mech.* 362, 1998, 273–295.
8. Nobuo Urata, Wave mode coupling and instability in the internal wave in aluminium reduction cells, *Light Metals* 2005, 455–460.